

Combinatorial measurements of Hall effect and resistivity in oxide films

J. A. Clayhold,¹ B. M. Kerns,¹ M. D. Schroer,¹ D. W. Rench,¹ G. Logvenov,²
A. T. Bollinger,² and I. Bozovic²

¹*Department of Physics, Miami University, Oxford, Ohio 45056, USA*

²*Brookhaven National Laboratory, Upton, New York 11973-5000, USA*

(Received 10 October 2007; accepted 3 March 2008; published online 21 March 2008)

A system for the simultaneous measurement of the Hall effect in 31 different locations as well as the measurement of the resistivity in 30 different locations on a single oxide thin film grown with a composition gradient is described. Considerations for designing and operating a high-throughput system for characterizing highly conductive oxides with Hall coefficients as small as 10^{-10} m³/C are discussed. Results from measurements on films grown using combinatorial molecular beam epitaxy show the usefulness of characterizing combinatorial libraries via both the resistivity and the Hall effect. © 2008 American Institute of Physics. [DOI: 10.1063/1.2901622]

I. INTRODUCTION

Recent advances in materials synthesis capabilities have created new challenges for measurements. In particular, the growing popularity and feasibility of combinatorial synthesis, in which a large number of distinct materials is grown simultaneously,^{1–5} has made it necessary to revisit many of the standard characterization techniques by speeding them up without sacrificing data quality. Indeed, the crucial need for new combinatorial characterization tools was recently highlighted in a special issue of Review of Scientific Instruments.⁶

Growth of atomically perfect epitaxial films by molecular beam epitaxy (MBE) has led to important new materials with useful properties. The MBE process lends itself naturally to combinatorial methods.^{7–10} The first combinatorial MBE (“COMBE”) system was constructed to grow oxide films in 1999 by Bozovic and co-workers^{7,8} at Oxxel GmbH, Bremen, Germany. The system is now at Brookhaven National Laboratory. The Oxxel/Brookhaven system relies on a very shallow incidence angle of the atoms arriving at the film surface from different directions to create a continuous composition spread across the wafer. A different scheme that relies on moving shutters was implemented by Tsui and He⁹ and used with success in studies of Ge-based magnetic semiconductors.^{11,12} By either technique, one can obtain films with controlled gradients in chemical composition. Lithography can be used subsequently to pattern from such a film a discrete set (a “combinatorial library”) of samples with a fine, position-addressable gradation of stoichiometry.

There is a pressing need for combinatorial methods appropriate to oxide materials. During the past two decades, a great number of novel oxides have been discovered that have important technological applications and show striking new physical behaviors. For many of these materials, especially the cuprate superconductors, the basic physics remains imperfectly understood. In addition, many new oxides have complicated phase diagrams, in which small variations in stoichiometry induce large changes of physical behavior. Creating precise combinatorial libraries of complex oxides

and characterizing them systematically will be an important undertaking. COMBE has solved one of these two problems—synthesis of arrays of single-crystal samples with well-controlled stoichiometry gradients. The second challenge, high throughput yet precise testing of their transport properties, is addressed here.

Among the most important characterization tools for conducting oxides are the measurements of electrical resistivity and Hall effect. The temperature dependence of the electrical resistivity can supply essential information about phase transitions (both electronic and structural), charge carrier dynamics, electron band structure, and the density of impurities. The Hall effect is particularly sensitive to the sign and density of charge carriers, Fermi surface topology, internal magnetization, and, in multiband systems, carrier dynamics. Together, these measurements reveal the complete resistivity tensor and are typically the first recourse for characterizing new conducting materials.

Previously, other authors have reported on systems for combinatorial resistance measurements alone in thin-film samples. Hewitt *et al.*¹³ recently described a useful system for combinatorial measurements of the dc resistivity in large-area metal films created using physical vapor deposition. We are interested in characterizing thin oxide films. A system for measuring the resistance of 62 different samples grown on a 10×10 mm² substrate was described in Ref. 10. We have found that adding a Hall effect capability changes nearly every aspect of the system design, including the probe, the electronics, and the data acquisition protocol. Here, we describe a system for high-throughput parallel measurements of the Hall effect and the resistivity in highly conductive thin oxide films as a function of temperature.

II. SYSTEM DESIGN CONSIDERATIONS

The size of the Hall signal is controlled by the carrier density, the sample resistance, and sample geometry. Hall effect voltages in our oxide films are small, typically a fraction of a microvolt in a 1 T magnetic field. With typical carrier densities on the order of 10^{22} cm⁻³, the Hall coefficient

cient R_H in standard units is on the order of $10^{-9} \text{ m}^3/\text{C}$. In units that are appropriate for acquiring the raw signal, we would have $R_H \sim 1 \text{ } \Omega \text{ nm}/\text{T}$, meaning that a sample with a thickness of 1 nm would have a Hall resistance of 1 Ω in a magnetic field of 1 T. For a typical sample with thickness of 100 nm, we find that we must limit the current to approximately 100 μA to avoid self-heating. Consequently, in a 1 T magnetic field, the signal will be 1 μV . Because the limit on total current scales with sample thickness, the maximum Hall signal will also be on the order of a microvolt for samples grown to other thickness. In fact, we will often need to measure certain highly doped materials, in which the Hall coefficient is an order of magnitude smaller than this estimate.

To resolve the Hall voltages, we need lock-in amplifiers with low-noise preamplifiers at the inputs. For an acceptable signal-to-noise ratio, we would like to have electronics that can resolve a few nanovolts. As discussed below, we find that we need to have separate measurement electronics for each individual sample so that for 31 samples, we need 31 separate lock-in amplifiers. Because of the large number of measurement channels, we found it most convenient to build the circuitry in house using circuit design software to lay out printed circuit boards. Surface-mounted electronic components facilitated production of the boards.

In highly conductive oxides, the Hall effect signal is much smaller than the resistance signal. The Hall angle, $\theta_H = \arctan(R_H H / \rho)$, where ρ is the resistivity and H is the magnetic field strength, is on the order of 10^{-4} at 1 T in the highly doped samples we are studying. The smallness of the Hall angle affects our system design parameters in many ways. Because of the small Hall angle, we need good contact alignment and measurements at many different field strengths to resolve the Hall effect. Misaligned contacts lead to a contribution to the measured voltage from the resistance. We use optical lithography to pattern the films and position the contacts accurately but when the Hall angle is 10^{-4} , there remain contributions to the measured voltage from the resistance of the film. The residual misalignment voltage can be eliminated by measuring the magnetic field dependence of the signal voltage. Another common way to eliminate the resistance voltage, the five-probe method with a compensating potentiometer, is less desirable because it is difficult to automate for 31 samples, requires additional contact pads and lines, and may introduce spurious effects from the potentiometers.

The requirement to measure at multiple field values slows the measurement down and ultimately makes it necessary to have separate data acquisition electronics for each of the 31 samples. Even if we were to use a single lock-in amplifier and a low-noise scanner to multiplex the signals for sequential measurement, the measurements would take too much time: we need to measure at low frequency, 37 Hz, to avoid phase shifts from stray capacitances at the contacts. For the Hall voltages, we set the lock-in amplifier to have a postintegration time constant of 2 s and we need to wait five time constants after switching channels before taking a reading. With 31 channels, the total time for taking data at a single magnetic field value is 3 minutes. Taking data at 11 different magnetic field values would require 30 min at a

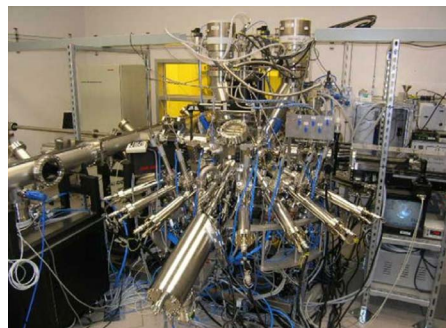


FIG. 1. (Color online) COMBE at Brookhaven National Laboratory. The growth chamber has 16 separate steep-angled sources with real-time flux monitoring on each channel. The sources can be paired to cancel stoichiometry gradients or controlled to create linear gradients. It is also possible to introduce gradients in the substrate temperature and/or in the oxidation power.

single temperature. If we then take data at 10 K intervals between 10 and 400 K, the total time required to characterize the wafer is 20 h—an order-of-magnitude longer than it took to grow the sample in the first place. In order to keep up with the rate of film growth, we need to have one lock-in amplifier per sample. In that case, the measurement time is limited only by magnetic field ramping and speed with which we can stabilize the temperature.

III. APPARATUS

A. Film growth

For this study, we have used a unique multichamber COMBE system at Brookhaven National Laboratory. The growth chamber (Fig. 1) contains 16 evaporation sources aimed at the substrate at a steep angle (20°) and provided with fast-acting pneumatic shutters. By using pairs of identical sources placed in opposite azimuth positions, i.e., with the atomic beam impinging at the same angle with respect to the substrate but from opposite sides, we can control the gradient of the corresponding atomic flux along the substrate. The maximum gradient (4% variation in deposition rate over a distance of 10 mm) is obtained when one source is open and its counterpart is closed, while a nearly zero gradient is achieved when both sources are open and emit the same atomic fluxes. The sample manipulator has six degrees of freedom (three translations and three rotations). It is provided with a sample heater with four individually controlled quartz lamps that allows for a temperature gradient to be profiled across the wafer. Oxidation under high-vacuum conditions is provided using a pure ozone supply system with four individually controlled nozzles, allowing for control of the oxidation-power gradient. This COMBE system therefore allows for position-addressable combinatorial variation of chemical composition, substrate temperature, and/or oxidation.

The source rates are monitored in real time by a custom-made 16-channel atomic absorption spectroscopy system. The spatial variations of rate can be mapped using a quartz-crystal oscillator monitor (QCM), mounted on a separate motorized and computer controlled manipulator with three translation degrees of freedom. A gradient in crystal structure

and morphology is monitored by a scanning reflection high-energy electron diffraction system capable of displaying 20 images taken in rapid succession and at the same incidence angle from different spots. A time-of-flight ion scattering and recoil spectroscopy system allows for real-time chemical analysis of the film surface with resolution high enough to clearly distinguish all the naturally occurring isotopes.

The system contains a second major vacuum chamber devoted to *in situ* lithographic processing, including ion-beam etching and electron-beam deposition of metallic and insulating layers. This chamber is installed in the clean room so that substrates can be prepared in a class-100 clean environment and loaded into the system without surface contamination. The growth chamber and the processing chambers are connected via a transfer chamber, and the samples can be transferred from one to another without breaking vacuum.

Altogether, this multichamber COMBE system allows one to deposit (combinatorial or uniform) thin films of complex oxides with atomic precision to analyze them in real time and to process them *in situ*. This has enabled reproducible synthesis of single-crystal films of LaSrCuO, BiSrCaCuO, and BaKBiO with rms surface roughness in the range of 0.2–0.5 nm. Furthermore, this technology allows fabrication of precise multilayers and superlattices and has enabled a series of novel physics experiments.^{14–18}

For the present study, we synthesized a number of thin films of $\text{La}_{2-x}\text{Sr}_x\text{CuO}_{4+\delta}$ with a large spread in the Sr doping level x along one chosen direction. A surface layer of gold was deposited *in situ* in the growth chamber to minimize the contact resistance.

B. Lithography and electrical contacts

Sample films are patterned in a class-100 clean room using optical photoresist and ion milling. The pattern is shown in Fig. 2. The current is directed down the center stripe, which is aligned with the one-dimensional stoichiometry gradient. In data presented here from measurements on $\text{La}_{2-x}\text{Sr}_x\text{CuO}_{4+\delta}$ (see the results in Sec. V), the current flowed in the direction of increasing strontium content. As described in the figure caption, voltages measured between pairs of the square contact pads yield values for either the Hall voltage or the resistance, depending on the pair chosen.

The processing of the films began with an initial lithographic stage that etched the pattern of Fig. 2 onto both the sample and top gold layer. Subsequently, the gold layer was removed from the central strip by masking off the contact pads and their electrodes, and then ion milling away the gold layer. Finally, everything but the contact pads was masked off and additional gold was evaporated onto the contact pads and leads to form mechanically robust contacts.

It is necessary for the combinatorial Hall/resistance studies to be able to mount and demount samples rapidly onto the cryostat probe. We use pogo pins—spring-loaded, gold-coated contact pins that have widespread use for rapid contacts in the semiconductor industry. In our case, it is crucial to emphasize that the pogo pins do not make the contacts—they merely facilitate the wiring (Fig. 3). Our electrical contacts are formed *in situ* in the growth chamber. The film to be measured is first capped with a highly conductive oxide layer

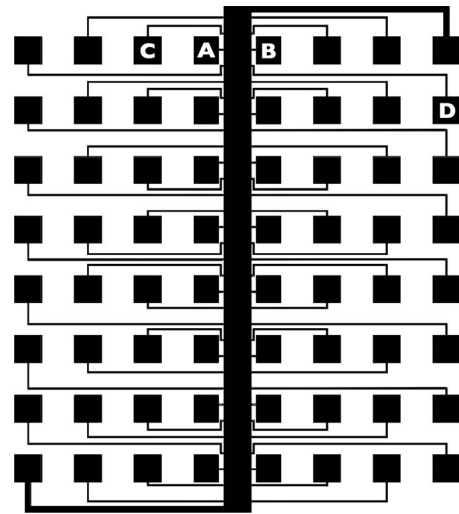


FIG. 2. Film lithography and contact pattern. The square contact pads are placed on a 1.1 mm grid. The current contacts are in the upper right and lower left corners of the pattern. The stoichiometry gradient is along the vertical axis—the Sr doping level increases in the sample from top to bottom. Contacts are made by *in situ* gold deposition onto a layer of highly conductive overdoped cuprate. Thirty-one distinct Hall effect voltage pairs make contact with the center stripe at equal spacings—the contacts labeled A and B form a Hall voltage pair. Commuting the leads with a multiplexer allows the measurement of the sample resistance at thirty equally-spaced locations—the pair of contacts C and A form a resistance voltage pair, as do B and D.

which is, in turn, coated with a gold layer, all within the growth chamber. During the patterning of the film, the highly conductive oxide layer and the gold layer are removed everywhere except at the square contact pads shown in Fig. 2. The quality of the contacts may be characterized during lithography, in the clean room, without the need for pogo pins because they are not the essential contact-forming connection. The square contact pads are purposely oversized to be much larger than the pogo pin contact head. The pogo pins themselves have a large range of vertical compressive motion—nearly 2 mm. We make use of the full range—when a sample is mounted, the pogo pins are compressed by nearly 2 mm. Consequently, when the sample holder is carefully

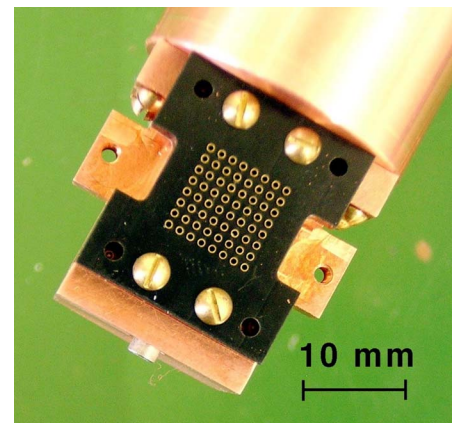


FIG. 3. (Color online) Receptacles for spring-loaded pogo pins on the cryostat tail. The 64-pin array with 1.11 mm spacing between adjacent pins makes contact with films etched into the pattern shown in Fig. 2. The four holes in the corners accept tapered guide pins on the sample holder, ensuring that the sample is mounted without lateral slippage.



FIG. 4. (Color online) Sample holder in place, mounted from the right and fastened with brass machine screws. Because the length of each pogo pin assembly is over 70% of the diameter of the tube, the wrap-around fastening arms were necessary to accommodate the available space.

machined, it becomes virtually impossible for the pogo pins not to engage the contact pads. All the dimensions on our sample holder were machined with tolerances finer than $25\ \mu\text{m}$. The sample holder (see Fig. 4) is fitted with tapered, vertical alignment pins. With a system that is so mechanically robust as ours, we have never had difficulty making connections between the gold contact pads and the pogo pins. Our experience regarding the reliability of pogo pins for connections to high-quality contacts accords with previous work.¹⁰

C. Cryogenics and magnetic field

The combinatorial Hall/resistance system was built for high throughput and low operational costs. Being able to sweep the magnetic field rapidly is crucial for throughput. Cryogen-free operation of the magnet reduces running costs. Both of these considerations led us to use an electromagnet to apply the magnetic field. We chose an electromagnet that, to accommodate our probe, has a gap between pole pieces of just under 50 mm but can attain a field strength exceeding 1 T.¹⁹ A gas-flow cryostat²⁰ is used to cool the sample with little vibration and low helium usage; it also allows for rapid mounting and demounting of samples.

Some care was necessary during the wiring of the probe. With as many copper wires as are needed for the combinatorial measurements, it would be easy to introduce a significant heat load onto the sample from the cryostat wiring. For this reason, we used quite fine (AWG 40) wire pairs, individually twisted, and formed into a single braid. As a result, the total thermal conductance through the wires is not a problem. We were nevertheless careful to heat sink the wires extensively before attaching them to the bottom of the probe. At the cold end of the probe, the wires wrap five times around a specially made copper cylinder which has an outer diameter of 30 mm and a length of 50 mm. The cylinder is controlled at the measurement temperature, ensuring that the wires are properly thermalized before making contact with the pogo pin receptacles.

D. Electronics

Electronics consist of the signal acquisition circuits, a multiplexer that permits us to interchange the voltage leads for measuring either the Hall effect or the electrical resistance and a current source. We found that it was convenient to use commercially available schematic capture and printed circuit board layout software for error-free routing of the many signals and for replicating the channel-specific circuitry. Using surface-mount electronic components wherever possible helped greatly to expedite final assembly. With surface-mount components, we were able to stencil-print solder paste, then use a pick-and-place machine to place the components, and finally employ a reflow oven for rapid, reliable soldering.

1. Signal acquisition

We fabricated separate analog signal acquisition circuitry, consisting of a preamplifier and a lock-in amplifier, for each pair of voltage contacts. A diagram of the signal acquisition circuit for a single channel is shown in Fig. 5. The differential signal voltage from a sample is amplified by a precision instrumentation amplifier U1 that has been hard-wired for a gain of 1000. The AD524 (Analog Devices) was a convenient choice for first-stage amplification because it has precision fixed gain settings, input protection, and a low noise rating of $7\ \text{nV}/\sqrt{\text{Hz}}$. The output of U1 goes through a single-pole high-pass filter to remove any dc offset before the next amplification stage. The buffers U2 and U3 are field-effect-transistor-input operational amplifiers with low input bias currents (typically 2 pA) to reduce the dc voltage that would otherwise exist across R1 from the bias currents at the inputs of the next amplifier. U4 is a programmable-gain instrumentation amplifier with fixed gain settings of 1, 10, 100, or 1000, selectable via a pair of digital inputs. U5 is a square-wave demodulator (AD630, Analog Devices) commonly used to make simple analog lock-in amplifiers. The circuit permits a choice of postintegration times, 0.2 or 2 s, depending on a transistor-transistor-logic (TTL)-level voltage at the noninverting terminal of U6. We typically use the longer time constant for Hall effect measurements and the shorter time constant for resistance measurements. The buffer U7 is only necessary because of an inconvenient low input impedance that can occur in the commercial multichannel analog-to-digital converter that we used to read the lock-in voltages.

The single-channel circuit described above was replicated 32 times onto eight different cards with four channels per card. A motherboard was made with eight slots for the cards. The motherboard not only routes the analog signals but also has digital lines for computer control of the gain of each channel and for choosing the postintegration time constant. The circuitry was built so that the gain setting for each channel could be individually selected, which would normally require 64 digital control lines from the computer. Incorporating four 16 bit shift registers onto the motherboard reduced the number of gain-control data lines.

We used 68-pin small computer system interface (SCSI) connectors to bring signals in from the cryostat and to send

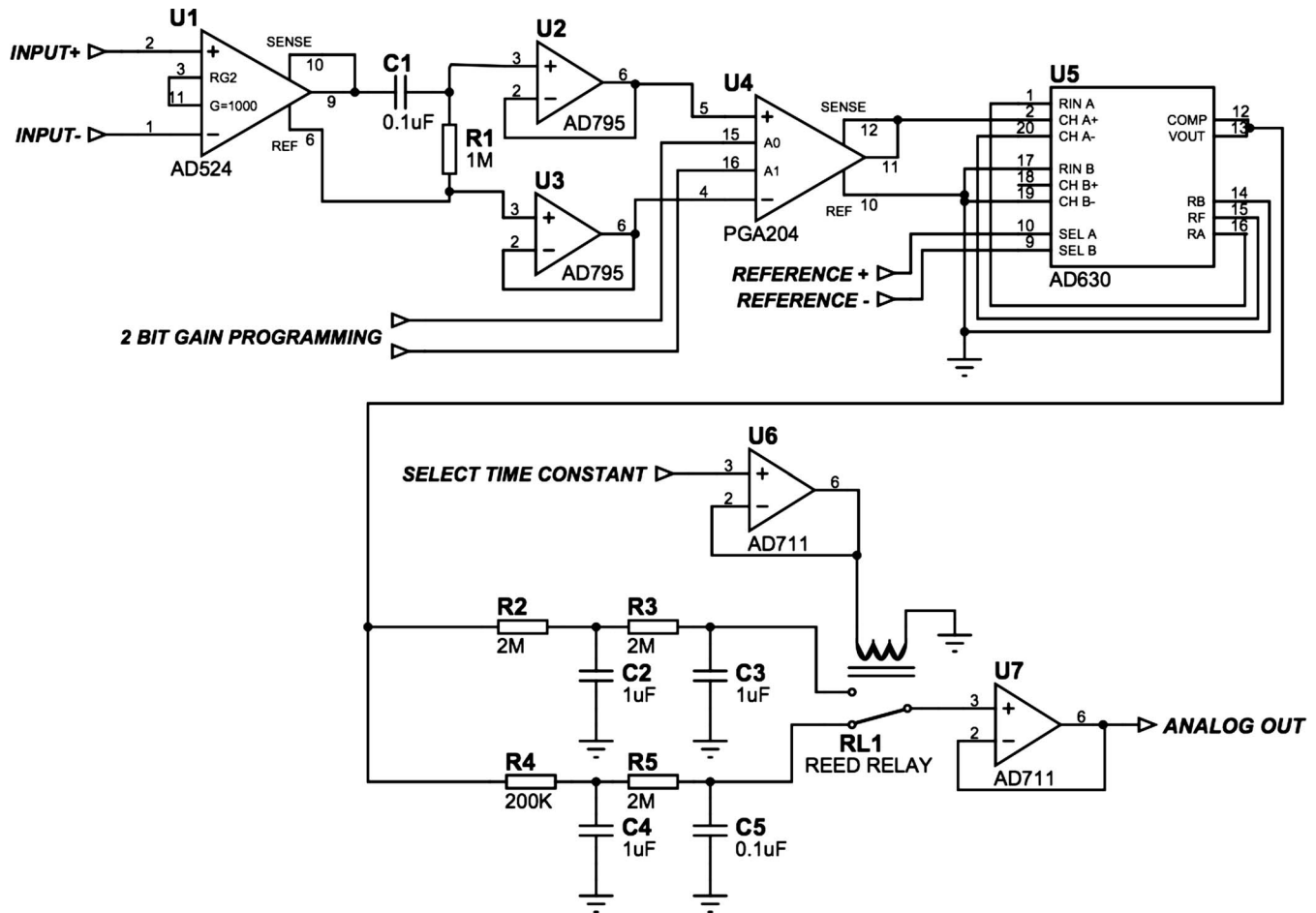


FIG. 5. Signal acquisition circuit (see text for details). The simple circuit was replicated 32 times, one for each sample measured, and was flexible enough to accommodate a wide range of samples for both Hall effect and resistance measurements.

signals out to the computer. The SCSI connectors were chosen because of the ready commercial availability of matching cables with 34 individually shielded twisted pairs. For the head of the cryostat, we fabricated a vacuum feedthrough from a SCSI connector mounted into a brass housing that was filled with epoxy.

2. Hall/resistance multiplexer

As shown in Fig. 2, the contacts to the film can be arranged for the measurement of either 31 Hall effect voltages or 30 resistance voltages, depending on the configuration of the voltage pairs. To facilitate the measurement of both Hall and resistance voltages, we made a specialized multiplexer to commute the signal connections between the two configurations. Because the current leads are the same for both Hall and resistance measurements, the multiplexer needed only to swap between two configurations of 62 signal wires. The multiplexer consisted of 62 different TTL-controlled, low-resistance single-pole, double-throw (SPDT) switches on a circuit board with signal inputs and outputs connected through board-mounted SCSI connectors. The circuit used 31 quad single-pole, single-throw (SPST) switches (ADG453, Analog Electronics) wired together as dual SPDT switches. The low on-resistance, 4Ω , of the switches is less than

the resistance of our cryostat wiring, so these switches are well suited as in-line elements for low-frequency ac measurements.

3. Current source

The sample excitation derives from a current source made from a commercial function generator driving a simple instrumentation-amplifier voltage-to-current circuit. There are three different current-setting resistors available, selected digitally using reed relays. With control of the function generator amplitude, the current is controllable over five orders of magnitude.

IV. DATA ACQUISITION

Using LABVIEW data control and acquisition software, the system was programed for computer control of the gain settings for each channel, the postintegration time, the amplitude and frequency of the current excitation, the state of the Hall/resistance multiplexer, the magnetic field strength and polarity, and the temperature set point. At each new temperature set point, the system waits for the temperature to stabilize, then initiates a sweep of 11 different field values between -1.1 and $+1.1$ T. At each field value, the system waits several postintegration time constants and then acquires the 31 Hall voltages. Upon returning to zero field, the

gains, current, and multiplexer are set for resistance measurement and the 30 resistance voltages are acquired. With samples that are more magnetoresistive, we would also measure the resistance voltages at each individual magnetic field value.

Good temperature stability is necessary for the Hall measurements. The resistance of the samples depends strongly on temperature, which means that the large resistance background signal from the contact offsets will fluctuate when the temperature fluctuates. For samples having a Hall angle of only 10^{-4} at our maximum magnetic field, we would like to have the temperature stabilized to within a few millikelvins of the set point. We use a gas-flow cryostat for fast sample mounting, low vibration, and quick turnaround, but gas flow cryostats can be difficult to control to high stability. The cryostat in our system has features to enhance stability, including cold gas shield flow around the helium transfer line, a needle valve, and flow impedances at the outlet.

V. RESULTS

Calibration of the multichannel signal acquisition electronics showed that the measurement resolution at our chosen frequency of 37 Hz, with 2 s postintegration time was on the order of 5 nV at the highest gain. There was no frequency dependence of the gain below 2 kHz for gains of 10^3 , 10^4 , and 10^5 . The highest gain setting, 10^6 , showed some frequency dependence above 200 Hz. The channel-to-channel gain showed negligible variations but we nevertheless performed a full calibration for each channel as a function of gain setting and frequency.

The contact resistances were typically a few ohms or less. The alignment of the transverse Hall contacts could be determined from electrical measurements at zero magnetic field. We found that 70% of the Hall contacts were aligned within $2\ \mu\text{m}$, roughly describable as a Gaussian distribution having an average offset of $-0.5\ \mu\text{m}$ and a standard deviation of $1\ \mu\text{m}$. The remaining 30% of the contacts had higher offsets, which presented no hindrance to resistance measurements but did affect Hall measurements in the samples with Hall angles as small as 10^{-4} at 1 T. A histogram showing a typical distribution of Hall offsets is in the inset of Fig. 6.

Resistivity and Hall effect results from measurements on a sample of the overdoped single-layer cuprate superconductor, $\text{La}_{2-x}\text{Sr}_x\text{CuO}_{4+\delta}$ are shown in Figs. 6 and 7. The film thickness was 975 Å and was lithographed with the pattern of Fig. 2. The width of the center current stripe was 300 μm , which is the same as the distance between adjacent resistance contacts. The room temperature resistance, measured with 150 μA current amplitude, was on the order of 20 Ω in each channel at room temperature. The resistivity followed a concave temperature dependence, $d^2\rho/dT^2 > 0$ (see Fig. 6), typical for overdoped cuprates. At room temperature, the resistivity varied from 2.191 to 2.114 $\mu\Omega\ \text{m}$, making a relative variation of 3.6% across the film.

Hall effect data are shown in Fig. 7. The inset shows the magnetic field dependence of the resistance between two Hall voltage contacts for a typical channel measured at 17 Hz with 250 μA current amplitude. The slope of the fitted

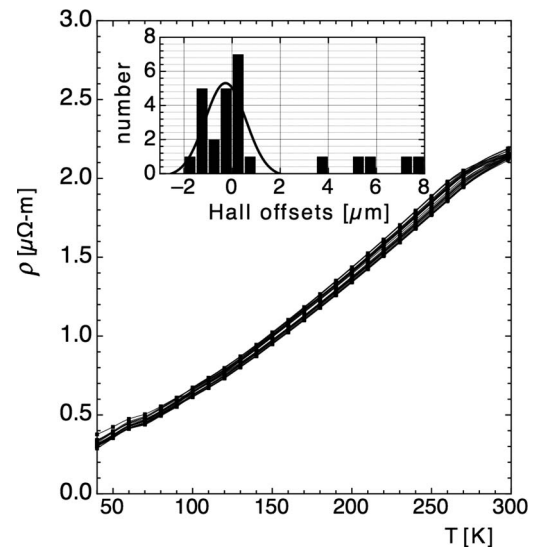


FIG. 6. Resistivity as a function of temperature. The resistivity decreases with increasing carrier concentration and had a total variation of 3.6% across the sample. The inset shows a histogram of the alignments of the transverse Hall contacts as measured in zero field. Most pairs are within $2\ \mu\text{m}$ as expected from optical lithography.

line corresponds to a Hall angle of 1.35×10^{-4} at 1 T. The background resistance signal from contact misalignment is just over nine times the variation of the Hall signal in 1 T field.

The temperature dependence of R_H is shown in the main panel of the figure. To minimize the effects of those channels that had large offsets and were sensitive to temperature fluctuations, the graph shows Hall coefficients for the channels, in which the ratio of the resistance background to the Hall signal was less than 10 and the error in the fitted Hall slope was less than 4%. We can see that the Hall effect in over-

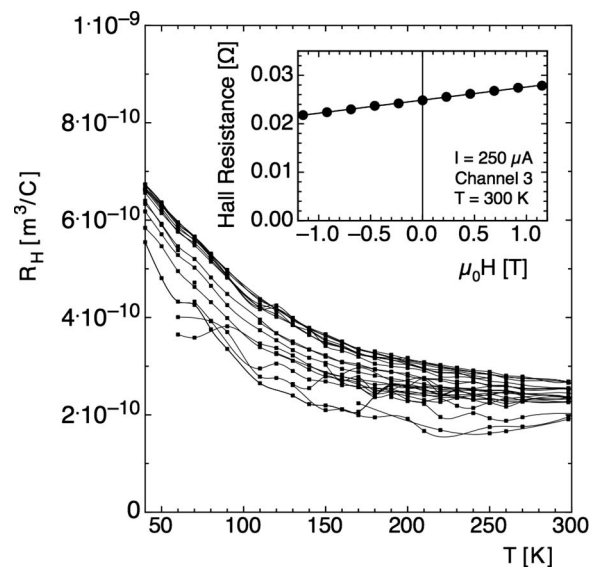


FIG. 7. Hall effect of $\text{La}_{2-x}\text{Sr}_x\text{CuO}_{4+\delta}$ as a function of temperature. The Hall coefficients for these overdoped samples with $x=0.222$ are nearly an order of magnitude smaller than in optimally doped material. The Hall coefficient drops rapidly with the carrier density at this value of x and shows a nearly 30% variation across the film. The curves serve to guide the eye. The inset shows the magnetic-field variation of the Hall resistance between two transverse contacts.

doped samples of $\text{La}_{2-x}\text{Sr}_x\text{CuO}_{4+\delta}$ is much more sensitive to changes of carrier density than is the resistivity. For $x > 0.2$, it is known that $R_H(x)$ drops to zero much faster than the $1/x$ dependence that would be expected for a single conduction band, where x is the carrier density. Indeed, the measured Hall coefficients of the samples shown in Fig. 7 are all on the order of $10^{-10} \text{ m}^3/\text{C}$, an order of magnitude smaller than is typical for underdoped or optimally doped cuprates.

The value of the Hall coefficient varies by almost 30% across the film. A comparison to previously reported Hall measurements²¹ on discrete bulk samples permits us to calibrate the carrier density. The data of Fig. 7 are consistent with a variation of x from 0.218 to 0.226 across the film, corresponding to a 3.6% relative variation of carrier density across the sample. This is consistent with the resistivity data as well as with the deposition-rate gradient ($\sim 4\%$ edge to edge) measured previously by scanning QCM. The high sensitivity of the Hall results to sample stoichiometry underscores the utility of the combinatorial Hall capability for studies of oxide films.

To summarize, we have built and operated a system for fabrication, processing, and simultaneous measurement of the resistance at 30 different locations and of the Hall effect at 31 locations on a single thin film grown with a combinatorial spread in chemical composition. The system was designed for rapid turnaround, the ability to accommodate resistive samples with small Hall coefficients, and for characterization of novel oxides with a very fine stoichiometry resolution.

ACKNOWLEDGMENT

This work has been supported by U.S. DOE Project No. MA-509-MACA.

- ¹X. D. Xiang, X. D. Sun, G. B. No, Y. Lou, K. A. Wang, H. Chang, W. G. Wallace-Freedman, S. W. Chen, and P. G. Schultz, *Science* **268**, 1738 (1995).
- ²G. Briceno, H. Chang, X. Sun, P. G. Schultz, and X.-D. Xiang, *Science* **270**, 273 (1995).
- ³H. Chang, I. Takeuchi, and X.-D. Xiang, *Appl. Phys. Lett.* **74**, 1165 (1999).
- ⁴R. B. van Dover, L. F. Schneemeyer, and R. M. Fleming, *Nature (London)* **392**, 162 (1998).
- ⁵T. Fukumura, M. Ohtani, M. Kawasaki, Y. Okimoto, T. Kageyama, T. Koida, T. H. Andd, Y. Tokura, and H. Koinuma, *Appl. Phys. Lett.* **77**, 3426 (2000).
- ⁶J. C. Grunlan, A. R. Mehrabi, and R. A. Potyrailo, *Rev. Sci. Instrum.* **76**, 062101 (2005).
- ⁷I. Bozovic and V. Matijasevic, in *Trends in Advanced Materials and Processes*, edited by D. P. Uskokovic, G. A. Battiston, J. M. Nedeljkovic, S. K. Milonjic, and D. I. Rakovic (Trans Tech, Staefa, Switzerland, 2000), Vol. 352, pp. 1–8.
- ⁸I. Bozovic, *IEEE Trans. Appl. Supercond.* **11**, 2686 (2001).
- ⁹F. Tsui and L. He, *Rev. Sci. Instrum.* **76**, 062206 (2005).
- ¹⁰G. Logvenov, I. Sveklo, and I. Bozovic, *Physica C* **460-462**, 416 9(2007).
- ¹¹F. Tsui, L. He, L. Ma, A. Tkachuk, Y. S. Chu, K. Nakajima, and T. Chikyow, *Phys. Rev. Lett.* **91**, 177203 (2003).
- ¹²F. Tsui, L. He, A. Tkachuk, S. Vogt, and Y. S. Chu, *Phys. Rev. B* **69**, 081304(R) (2004).
- ¹³K. C. Hewitt, P. A. Casey, R. J. Sanderson, M. A. White, and R. Sun, *Rev. Sci. Instrum.* **76**, 093906 (2005).
- ¹⁴I. Bozovic, G. Logvenov, I. Belca, B. Narimbetov, and I. Sveklo, *Phys. Rev. Lett.* **89**, 107001 (2002).
- ¹⁵P. Abbamonte, L. Venema, A. Rusydi, G. A. Sawatzky, G. Logvenov, and I. Bozovic, *Science* **297**, 581 (2002).
- ¹⁶I. Bozovic, G. Logvenov, M. A. J. Verhoeven, P. Caputo, E. Goldobin, and T. H. Geballe, *Nature (London)* **422**, 873 (2003).
- ¹⁷I. Bozovic, G. Logvenov, M. A. J. Verhoeven, P. Caputo, E. Goldobin, M. R. Beasley, and T. H. Geballe, *Phys. Rev. Lett.* **93**, 157002 (2004).
- ¹⁸N. Gedik, D.-S. Yang, G. Logvenov, I. Bozovic, and A. Zewail, *Science* **316**, 425 (2007).
- ¹⁹Model 3473-70 dipole electromagnet, GMW Associates, 955 Industrial Road, San Carlos, CA 94070.
- ²⁰Model Helitran LT-3 open cycle cryostat, custom length tail for electromagnet, Advanced Research Systems, 7476 Industrial Park Way, Macungie, PA 18062.
- ²¹H. Y. Hwang, B. Batlogg, H. Takagi, H. L. Kao, J. Kwo, R. J. Cava, J. J. Krajewski, and J. W. F. Peck, *Phys. Rev. Lett.* **72**, 2636 (1994).